X-ray nanofocusing by kinoform lenses: A comparative study using different modeling approaches

Hanfei Yan
National Synchrotron Light Source II, Brookhaven National Laboratory, Upton, New York 11973, USA
(Received 2 June 2009; revised manuscript received 17 August 2009; published 1 February 2010)

We conduct a comparative study on various kinoform lenses (KLs) for x-ray nanofocusing by using the geometrical theory, the dynamical diffraction theory, and the beam propagation method. This study shows that the geometrical theory becomes invalid to describe the performance of a KL for nanofocusing. The strong edge diffraction effect from individual lens element, which distorts the desired wave field, leads to a reduction in the effective numerical aperture and imposes a limit on how small a focus a KL can achieve. Because this effect is associated with a finite thickness of a lens, larger lens thickness depicts a stronger distortion. We find that a short KL where all lens elements are folded back to a single plane shows an illumination preference: if the illuminating geometry is in favor of the Bragg diffraction for a focusing order, its performance is enhanced and vice versa. We also find that a short KL usually outperforms its long version where all lens elements do not lie in a single plane because the short one suffers less the wave field distortion due to the edge diffraction. Simulation results suggest that for a long KL, an adaptive lens design is needed to correct the wave field distortion in order to achieve a better performance.

DOI: 10.1103/PhysRevB.81.075402 PACS number(s): 41.50.+h, 42.25.−p, 61.05.cc

I. INTRODUCTION

The difficulty in fabricating x-ray focusing lenses with high numerical aperture (NA) is the major obstacle of advancing the resolution of x-ray microcopy into the nanometer scale. In the last decade, a variety of optics utilizing reflective, refractive, and diffractive properties of x-rays has been explored to achieve a small focus and has yielded up to date a focal size ranging from 15 to 50 nm.[1–7] Among them, diffractive optics are most promising to deliver true nanometer focus since their NA is not limited by the critical angle of the lens material for x rays. Theoretical studies have shown that multilayer Laue lens (MLL), a type of diffractive optics, is in principle capable of achieving even atomic resolution (<1 nm).[8] Recently, Kinoform lenses (KLs) received increasing attentions for x-ray nanofocusing due to their ability of bending all incoming photons (assuming no absorption) into one single focus.[9–14] Because a KL is a hybrid optic possessing both refractive and diffractive properties, a question arises whether KLs are capable of achieving nanometer focus. Most of the prior theoretical studies on KLs were carried out in the framework of the geometrical optics,[15–17] which does not take into account the diffraction effect inside the optic and fails when the lens is thick or the diffractive element of the lens is small. Obviously, a full-wave theory must be employed to evaluate the performance of thick KLs with high NA. This knowledge not only tells us the theoretical focusing limit of KLs, but also the way to optimize their performance.

In this paper, we applied the geometrical theory, the dynamical diffraction theory, and the beam propagation method to perform a comparative study on various KLs. The latter two methods are both wave theory based. Applicability and limitations of these methods are discussed. We find that for a short KL where all the elements are folded back into a single plane, it can be treated as a blazed zone plate; it has multiple foci and possesses a similar focusing limit with MLLs with flat zones. In such cases, the diffractive property of the KL is dominant and the Bragg condition plays a critical role in determining the lens' effective NA. An interesting phenomenon revealed by simulations is that the short KL exhibits an orientation preference for illumination: when its sawtooth-like surface is illuminated by a plane wave, the focusing performance is much better than that when its flat surface is illuminated. This phenomenon is a result of the Bragg diffraction and will diminish as the NA decreases.

For a long KL where lens elements do not lie in a single plane, we find it has only one single focus, a great advantage compared to its short version. However, the strong diffraction from steep edges will cause a severe aberration on the wave field propagating through the lens and leads to a significant reduction in the effective NA. The focusing performance of a long KL is usually worse than its short counterpart because of this effect. This study suggests that in order to achieve a smaller focus, a subsequent element in a long KL has to be designed adaptively to compensate the phase aberration of the wave front caused by the edge diffraction in a preceding element.

II. GEOMETRICAL THEORY

An x-ray plane wave can be focused by a concave refractive lens as shown in Fig. 1, in which the optical path difference for different rays to its focus is compensated by the phase advance they experience inside the lens material. The emerging wave from the lens, therefore, interferes constructively at its focus. For such a concave-plano lens, if we neglect the refraction that occurs on the concave surface, the thickness profile of the lens is simply written as

$$\Delta z(x) = (\sqrt{x^2 + f^2} - f)/\delta, \tag{1}$$

where f is the focal length and δ is the difference of the refractive index of the lens material from unity. In general, the refractive index is a complex number

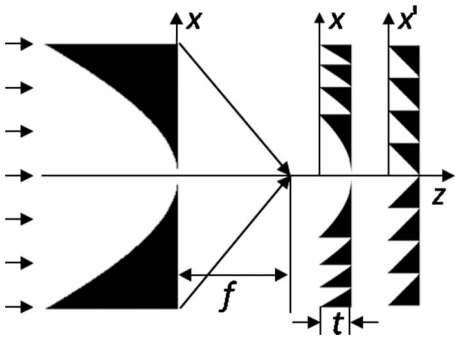

FIG. 1. A concave-plano refractive lens with parabolic profile to focus a plane wave (left), the corresponding KL with excessive materials removed (middle), and the periodic triangle array after a variable transform (right).

$$n = 1 - \delta + i\eta, \tag{2}$$

where the imaginary component, η, corresponds to the absorption. We can also write

$$\chi = -2\delta + 2i\eta, \tag{3}$$

where χ is the susceptibility function.

A major factor that limits the achievable NA of a refractive lens is its absorption: the outer part of the lens quickly becomes too thick to allow x rays to penetrate. The impact of absorption can be reduced by removing excessive materials where the corresponding phase variation is an integer multiple of 2π, so that the emerging waves still add up in phase at the focus. The lens is then divided to many sawtoothlike elements (zones) known as KLs.

If all elements are folded back to a single plane, forming a short KL as shown in Fig. 1, the thickness profile of a zone is then determined by the equation

$$\Delta z_j(x) = (\sqrt{x^2 + f^2} - \sqrt{x_j^2 + f^2})/\delta, \tag{4}$$

where x_j corresponds to the start position of the jth zone. Because an integer multiple m of 2π phase shift occurs at each x_j, we can derive

$$j(m2\pi) = 2\pi\Delta z(x_j)\delta/\lambda, \tag{5}$$

where λ is the wavelength of the incident x ray. Substituting Eq. (1) into Eq. (5), we obtain

$$j(m\lambda) = \sqrt{x_j^2 + f^2} - f \tag{6}$$

or

$$x_j^2 = 2j(m\lambda)f + j^2(m\lambda)^2. \tag{7}$$

One may recognize that Eq. (7) is essentially the zone plate law. Thus, a short KL possesses both refractive and diffractive properties and can be treated as a blazed zone plate with a special zone structure. Instead of having alternating layers, a short KL has zones shaped to match the exact phase change needed for forming a spherical wave front. Each zone serves as a refractive lens while the way the zones are arranged follows the zone plate law. For a short KL with high NA and a large number of zones, one expects that the diffractive property prevails since the waves emerging from all zones have to be in phase at the focus; the arrangement of zones is more important than the shape of the zone. An interesting question arises as to how small a beam a short KL can focus x rays to since the diffraction effect may impose a limit on its achievable NA.

Most of prior theoretical studies on KLs were carried out in the framework of the geometrical theory, which assumes the transmission function of the lens can be calculated directly from its thickness profile. Following the method described in Ref. 15, here we give a brief derivation of the efficiency equation. For an incident plane wave, the exit wave field from a short KL is

$$E_{geo}(x) = \exp(ikt)\exp[ik(n-1)\Delta z_j(x)], \tag{8}$$

where $k = 2\pi/\lambda$ is the wave number and t is the thickness of the KL (see Fig. 1). The constant phase factor, $\exp(ikt)$, is of no importance and will be neglected in the following discussion. Applying the variable transform

$$x' = \sqrt{x^2 + f^2} - f, \tag{9}$$

we can see that the exit wave field becomes periodic in terms of x',

$$E_{geo}(x') = \exp[ik(n-1)(x' - x_j')/\delta], \quad x_j' = j(m\lambda). \tag{10}$$

One then expands $E_{geo}(x')$ into a Fourier series

$$E_{geo}(x') = \sum_{h=-\infty}^{\infty} E_h \exp(ihkx'/m),$$

$$E_h = \frac{\exp(-2\pi m\varepsilon) - 1}{i2\pi(-m - h + im\varepsilon)}, \quad \varepsilon = \eta/\delta,$$

$$h = 0, \pm 1, \pm 2, \pm 3, \ldots . \tag{11}$$

Consequently, we can express the exit wave field as

$$E_{geo}(x) = \sum_{h=-\infty}^{\infty} E_h \exp[i\phi_h(x)], \quad \phi_h(x) = hk(\sqrt{x^2 + f^2} - f)/m. \tag{12}$$

Each wave component, $E_h \exp[i\phi_h(x)]$, corresponds to a spherical wave with constant amplitude converging to (or diverging from) the hth order focus of the short KL. It is evident that when the focusing order has $h=-m$, it reaches a maximum efficiency

$$c_{-m} = \left| \frac{\exp(-2\pi m\varepsilon) - 1}{2\pi m\varepsilon} \right|^2, \tag{13}$$

which is one if there is no absorption ($\varepsilon=0$). Thus the negative-mth order focus of a short KL is its principal focusing order. One shall note here a focusing order has a negative sign, different from the usual convention where a positive sign corresponds to a focusing order. The focusing efficiency of an arbitrary order can be written as

$$c_h = \frac{[\exp(-2\pi m\varepsilon) - 1]^2}{4\pi^2[(m+h)^2 + m^2\varepsilon^2]}. \quad (14)$$

We want to emphasize that in deriving Eq. (13), the thickness t is assumed to be $m\lambda/\delta$ and the maximum phase variation in one zone is $m2\pi$.

III. TAKAGI-TAUPIN DESCRIPTION OF DYNAMICAL DIFFRACTION THEORY

The geometrical theory neglects the diffraction effect and is invalid when the zone becomes very small or the thickness t is large. In the following, we employ the recently developed Takagi-Taupin description of dynamical diffraction theory[8] (thereafter denoted TTD) for diffractive optics to investigate the possible focusing limit for short KLs.

Similar to Eq. (12), we write the wave field in the lens as a superposition of many diffraction orders

$$E_{dyn}(x,z) = \sum_h E_h(x,z)\exp[ik\vec{s}_0 + i\phi_h(x)], \quad (15)$$

where $\vec{s}_0$ is a unit vector along the incident wave direction and $\phi_h(x)$ is defined in Eq. (12). The amplitude of the hth order is now a function of positions satisfying the following central differential equation (assuming σ polarization):

$$\frac{2i}{k}\nabla E_h\left(\vec{s}_0 + \frac{\nabla\phi_h}{k}\right) + \beta_h E_h + \sum_{l=-\infty}^{\infty}\chi_{h-l}E_l = 0,$$

$$\beta_h = i\frac{\nabla^2\phi_h}{k^2} - 2\vec{s}_0\frac{\nabla\phi_h}{k} - \left(\frac{\nabla\phi_h}{k}\right)^2. \quad (16)$$

In Eq. (16), χ_h is the pseudo-Fourier coefficient of the susceptibility function of the short KL

$$\chi_{\mathrm{KL}}(x,z) = \sum_h \chi_h(z)\exp[i\phi_h(x)]. \quad (17)$$

Utilizing the same variable transform in Eq. (9), we can transform a short KL into a periodic structure with period $m\lambda$ and triangle zones as shown in Fig. 1. For this periodic structure, we can deduce the expression of $\chi_h(z)$,

$$\chi_0(z) = \frac{z}{t}\chi, \quad \chi_{h\neq 0}(z) = \frac{\chi[\exp(i2h\pi z/t) - 1]}{2ih\pi}. \quad (18)$$

Substituting Eq. (18) into Eq. (16), we can calculate the amplitude function for all orders.

To explore the possible focusing limit, we start by considering a short KL made of silicon. It has a radius of 40 μm in x direction and a focal length of 10 mm, illuminated by a plane wave with unity amplitude at 11.3 keV. We assume the thickness of the KL corresponds to a 2π phase shift. Therefore, one has $m=1$ and $t=28.8$ μm. Because of the plane wave illumination, the boundary conditions are

$$E_0(x,0) = 1, \quad E_{h\neq 0}(x,0) = 0. \quad (19)$$

By solving Eq. (16), we show in Fig. 2 the variation of the local diffraction intensity of the principal focusing order ($h=-1$) as a function of radius x on the exit surface,

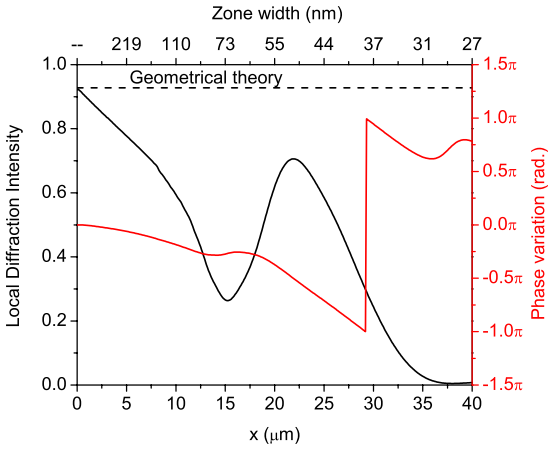

FIG. 2. (Color online) Local diffraction intensity of the negative-first order and its phase on the exit surface of the KL.

$|E_{-1}(x,t)|^2$. It can be seen that only in the close vicinity of the center ($x\sim 0$) TTD agrees with the geometrical theory. Instead of being a constant over the radius, which is predicted by the geometrical theory, the local diffraction intensity calculated by TTD declines quickly as x is away from the center. In this particular case, for positions with zone width smaller than 30 nm ($x>35$ um), we can see that the local diffraction intensity drops down to nearly zero; beyond this position, the lens does not contribute to focusing anymore. Therefore, the effective NA of this lens is smaller than its physical NA. More specifically, we expect a focusing limit for this type of KLs since increasing their physical radius will not increase the effective NA. In addition to the diffraction intensity variation, a phase variation of the amplitude function across the radius can also cause significant aberrations on the focus and result in a decrease of the effective NA, so we plotted it in Fig. 2 as well. A phase change over π is observed around $x=29$ μm, which indicates that diffracted waves emerging from positions beyond this point will interfere destructively with those from inner positions, resulting in a further reduction in the effective NA.

For a better understanding of how the diffraction physics changes from the regime where the geometrical theory is valid to the regime where a full-wave dynamical theory has to be applied, the two-dimensional (2D) intensity distributions of the actual wave field (superposition of all diffraction orders) inside the short KL around $x=2$ and 22 μm are depicted on the top panel of Figs. 3(a) and 3(b), respectively. The bottom panel shows the one-dimensional (1D) intensity variation of the wave field on the exit surface calculated by TTD and the geometrical theory, together with the zone profile. Near the center ($x=2$ μm), the zone width is large and the structure is less periodic. In the middle of such broad zones, the difference between two calculation methods is negligible. However, an interesting phenomenon is observed from the TTD calculation: near these steep edges of the zones, the wave field intensity oscillates significantly, showing a deep valley on one side and a strong peak on the other side of the edge. The oscillation diminishes with the distance to the edge. This is very different from what the geometrical calculation predicts, which assumes a sharp change of the

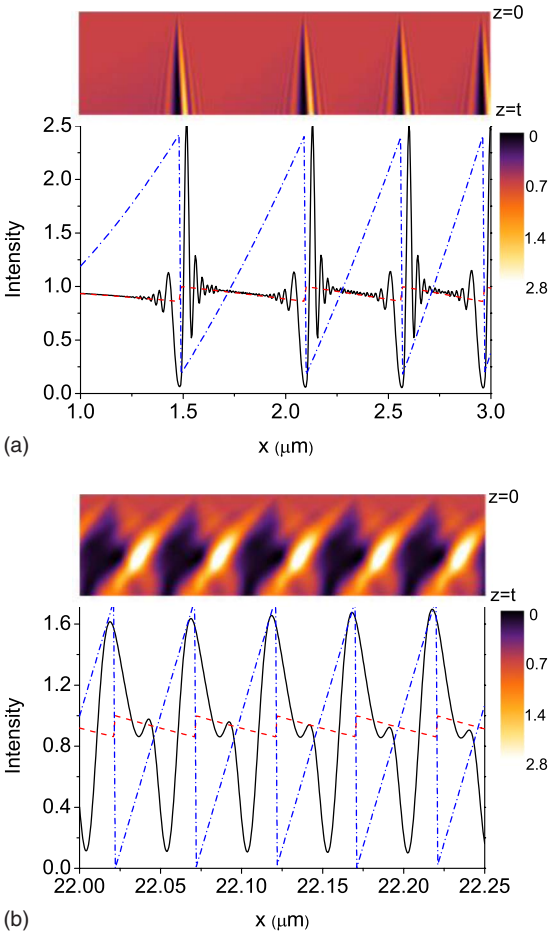

FIG. 3. (Color online) 2D intensity distribution of the wave field inside the KL (top) and the 1D wave field intensity variation on the exit surface at $z=t$ (bottom) around (a) $x=2$ μm and (b) $x=22$ μm. The 1D curves are the zone profile (blue dash-dotted), the wave field intensity variation calculated by the geometrical theory (red dashed), and by the dynamical diffraction theory (black solid).

intensity across the edge. These interference fringes are caused by the wave-guide effect of a slit with finite thickness. We note that similar effect was widely studied in proximity x-ray lithography.[18–21] In general, the edge diffraction distorts the desired converging wave field and degrades the focusing performance of a lens. Because it is associated with a finite thickness, we expect that this effect becomes more pronounced as the thickness t increases.

As we can see, near the center of a short KL, the geometrical theory is a good approximation to the more rigorous dynamical diffraction theory, except for regions close to steep edges. In other words, in the vicinity of the center, the KL behaves more like a refractive lens and its diffractive property is minor. However, this does not hold as the zone width shrinks. The 2D intensity distribution around $x=22$ μm shown in Fig. 3(b) looks completely different from that shown in Fig. 3(a), although based on the geometrical theory the two patterns should resemble each other. This indicates that around this position, diffraction becomes dominant and the simple geometrical theory is no longer valid. The 1D intensity variation of the wave field on the exit

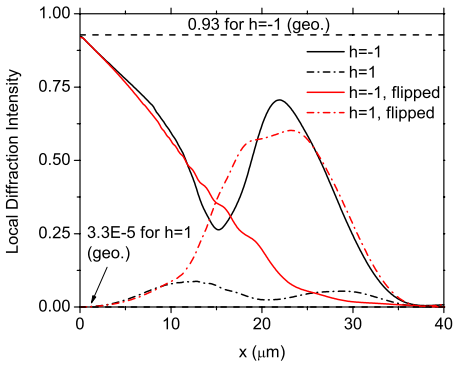

FIG. 4. (Color online) The local diffraction intensity variation of the positive-first and the negative-first orders of the short KL in concave-plano and planoconcave (flipped) geometries. For a comparison, the values calculated by the geometrical theory are also shown.

surface clearly shows the difference between two calculations. These two results deviate significantly not only near steep edges but also in the middle of the zones. Obviously, there would be enormous errors if one employs the geometrical theory to calculate the wave field in this region.

Another interesting question one may ask is whether the performance will be different if the flat surface of the short KL is illuminated, i.e., flip it horizontally. From the viewpoint of the geometrical theory, there should be no difference since the optical path is not changed after flipping, but it may not be the case if we take into account the diffraction effect. Since the structure is not symmetric about the x axis, intuitively we will expect a difference. For the flipped geometry, Eq. (18) is rewritten as

$$\chi_0(z) = \left(1 - \frac{z}{t}\right)\chi, \quad \chi_{h\neq 0}(z) = \frac{\exp[i2h\pi(1 - z/t)] - 1}{2ih\pi}\chi. \tag{20}$$

Substituting into Eq. (16), one can solve all diffraction orders. As a comparison, in Fig. 4 we plot the local diffraction intensity of diffraction orders $h=\pm 1$ in both concave-plano and planoconcave (flipped) geometries. We can see in the former case the positive-first order, which corresponds to a divergent spherical wave, has a negligible intensity compared to that of the negative-first order. In the latter case, however, the situation is reversed; the negative-first order in the outer part is significantly suppressed while the positive-first order is strongly enhanced. Since the optical path is not changed when the short KL is flipped, this change is solely due to the diffraction effect. We attribute this phenomenon to the Bragg diffraction after the speculation on the geometry. In the concave-plano case, the sawtoothlike surface of the short KL is facing to the incident plane wave. The incidence angle with respective to this surface is in favor of the Bragg diffraction for the negative orders, which is desirable. On the other hand, in the planoconcave case, this angle is in favor of the Bragg diffraction for the positive orders, which is not wanted. For the negative orders, they deviate from the Bragg condition further and are suppressed. Clearly, for a better focusing performance, the former geometry is preferred. One

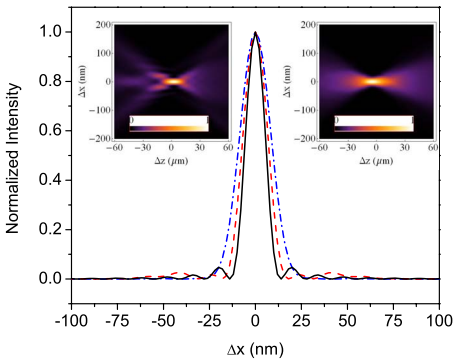

FIG. 5. (Color online) Focus profiles in the concave-plano (red dashed) and planoconcave (blue dash-dotted) geometries. The diffraction-limited focus is also plotted (black solid) for comparison. Intensity is normalized. Inserts show the intensity distribution around the focus in the concave-plano (left panel) and planoconcave (right panel) geometries.

may notice that in the vicinity of the center where the diffraction effect is weak, there is no much difference for these two geometries. Figure 5 shows focus profiles in these two cases together with the diffraction-limited focus. It can be seen that the concave-plano geometry yields a focus of 14.7 nm (full width at half maximum, FWHM), smaller than that of 19.2 nm for the planoconcave geometry. However, it is still larger than the diffraction-limited focus of 11.6 nm due to the fact that the effective NA is smaller than the physical NA as we discussed earlier.

It has been shown that there can be an integer multiple (m) of 2π phase variation in each zone since the phase relationship of the emerging wave front is still preserved. Because the zone width is proportional to m, a large m number will greatly alleviate the difficulty of fabricating small zones in practice, but with a price of efficiency; the thickness is also proportional to m so the absorption increases as well. From the viewpoint of the geometrical theory, no other adverse effect is foreseen. However, it may not be true because the diffraction effect has to be taken into account.

In Fig. 6 we plot the local diffraction intensity of the principal focusing order ($h=-m$) when m is equal to 1, 2, 3, 4, and 8, corresponding to a thickness t of 28.8, 57.6, 85.6,

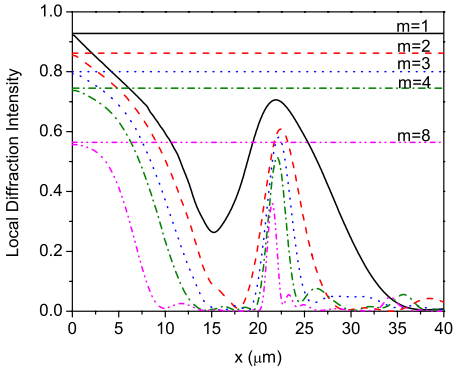

FIG. 6. (Color online) The local diffraction intensity variation of the principal focusing order when $m=1$, 2, 3, 4, and 8. The horizontal flat lines correspond to the values calculated by the geometrical theory.

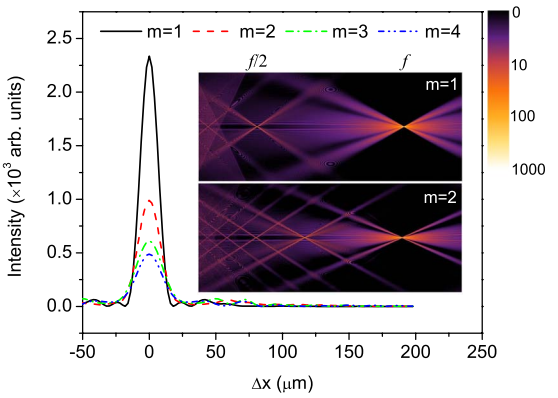

FIG. 7. (Color online) Focus profiles for $m=1$, 2, 3, and 4. Inset shows the intensity distribution (on logarithm scale) after the KL for $m=1$ and 2.

115, and 230 μm, respectively. One shall bear in mind that a short KL has both refractive and diffractive properties. According to Eq. (7), it can be seen that the nominal focal length for a short KL is mf, so we expect foci at mf/h. Only at these positions do the waves from individual zones add up in phase. For individual zones serving as refractive lenses, however, the transmitted wave only converge to the focus at f. As a result for a short KL, the negative-mth focusing order is the principal one, different from other diffractive optics where usually the first-order focus achieves the maximum efficiency.

From the simulation results shown in Fig. 6, we can see that the performance of the KL degrades as m increases. Not only the local diffraction intensity drops down as expected, but also the effective NA is reduced. For a large m value, the local diffraction intensity decreases to nearly zero much faster than that for a small m value, i.e., qualitatively speaking, the effective NA is inversely proportional to m. This may be due to a stronger wave-guide effect as t increases. We notice that the diffraction intensity near the center suffers less change in comparison to the value calculated by the geometrical theory as m increases. Thus if we only utilize the central part of the KL with a small NA, using a large m reduces the focusing efficiency but it has little effect on the focal size because the effective NA is barely affected. When the diffraction property becomes dominant as the NA increases, however, a large m that corresponds to a larger outmost zone width will lead to a broader focus.

Another adverse effect of using a large m is the presence of additional foci. The insets in Fig. 7 show the intensity distribution after a short KL in the cases of $m=1$ and 2. When $m=1$, there is no other foci between f and $f/2$. In the case of $m=2$, an additional focus appears at the position of $2f/3$. Due to the fact that a short KL can be treated as a blazed zone plate, foci at mf/h will show up. Figure 7 depicts the principal focus line profiles for different m values. When m is increased, the principal focus suffers not only a reduction in intensity but also a broadening in the peak width, changing from 14.7 nm for $m=1$ to 22.8 nm for $m=4$. As a result, it is not desirable to increase m number if one wants to achieve a small beam size.

IV. BEAM PROPAGATION METHOD

The TTD described in Sec. III is in favor of Bragg diffraction, i.e., the more periodic the structure is, the easier a solution can be found. A KL, like all other diffractive optics, is least periodic in the center. For the inner zones and a large m number, the TTD starts to lose its computational advantage compared to other modeling methods because a great number of high orders of diffraction have to be included in the calculation in order to achieve a high accuracy. In addition, for long KLs where zones do not lie in a single plane, the TTD becomes difficult to apply. To tackle these problems, in the following, another wave-propagation-based modeling approach, the beam propagation method (BPM),[22] will be employed. BPM has been widely used to study the edge diffraction effect in x-ray proximity lithography.[19,20] Here we will give a brief description of this method.

Consider that the optic consists of many thin slices with small thickness Δz. If the wave field on the front surface of a slice, $E(x,y,z)$, is known, the zero-order approximation of the wave field on its back surface, $\tilde{E}(x,y,z+\Delta z)$, can be calculated by free-space propagation (vacuum, $\chi=0$)

$$\tilde{E}(x,y,z+\Delta z) = \frac{1}{4\pi^2}\int\left\{\exp[i(k_x x + k_y y) + ik_z \Delta z]\int E(x,y,z) \times \exp[-i(k_x x + k_y y)]dxdy\right\}dk_x dk_y,$$

$$k_z = \sqrt{k^2 - k_x^2 - k_y^2}. \tag{21}$$

Then the correction on the wave field due to the presence of the optic can be written as

$$E(x,y,z+\Delta z) = \tilde{E}(x,y,z+\Delta z)\exp[ik\chi(x,y,z)\Delta z/2]. \tag{22}$$

Repeating this computation process for all slices, we can propagate the wave field from the entrance surface of an optic to its exit surface. One shall note the paraxial approximation is applied in BPM and χ has to be small. The latter is easy to be satisfied in the x-ray domain. Another approximation made in BPM is that the back reflection is negligible. Thus, BPM is suitable to calculate the wave field in an x-ray optic with an arbitrary structure in the forward propagation scheme and with a small NA.

As a comparison, we calculate the wave field on the exit surface using BPM in a region close to the center of the short KL studied in Fig. 3(a). The result is shown in Fig. 8. We can see the BPM and the TTD yield the exactly same result. In this case, the TTD still outperforms the BMP in terms of computation time so one gains no benefit by employing the latter one. For long KLs where zones do not lie in the same plane, however, the BPM is much easier to be implemented.

In the example below, we apply the BPM to investigate the performance of a Si KL with a focal length of 10 mm and a radius of 11 μm. It is operated at energy of 11.3 keV and has $m=8$, so that each zone has a thickness of 230 μm along the optical axis. Four geometries are studied, shown in Fig. 9. In the first two cases, the different side of a long KL is illuminated by a plane wave. As a comparison, we also study in the latter two cases a short KL with its two sides illuminated by a plane wave. Ideally, these four geometries should give the same diffraction-limited focal size of 41.8 nm (FWHM) since their physical NAs are the same. But the simulation indicates it is not the case. Figure 10 depicts the line focus profiles for all four geometries, together with their 2D intensity distributions around the focus (insets). As can been seen, in all cases which side of the lens is illuminated has little effect on its performance. This is because here the NA is very small (1.1×10^{-3}) and the Bragg diffraction is not strongly excited; the preference on illumination shows up only when the Bragg diffraction becomes dominant. The short KL in cases iii and iv outperforms the long KL in cases i and ii, producing a more intense and smaller focus. The FWHMs of the focus are 83.5, 74.3, 57.0, and 61.5 nm in cases i, ii, iii, and iv, respectively. We attribute the performance degradation of the long KL to the edge diffraction effect. The top panel in Fig. 11 shows the wave field intensity distribution inside a long KL for case i. Strong interference fringes are observed along the steep edge of each diffractive element, distorting the wave propagating to the next adjacent element. Because the lens is designed to reconstruct a plane wave front to a converging spherical wave front, any

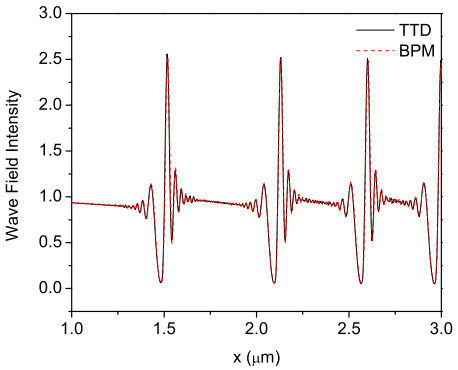

FIG. 8. (Color online) A comparison of the results calculated by the dynamical diffraction theory (TTD) and the BPM. The KL studied is the same with the one shown in Fig. 3(a).

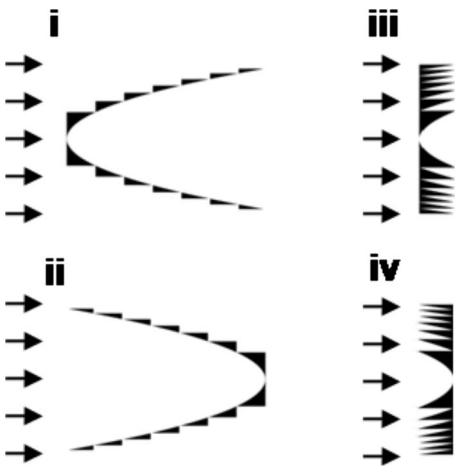

FIG. 9. Long and short KLs with the same radius illuminated by a plane wave.

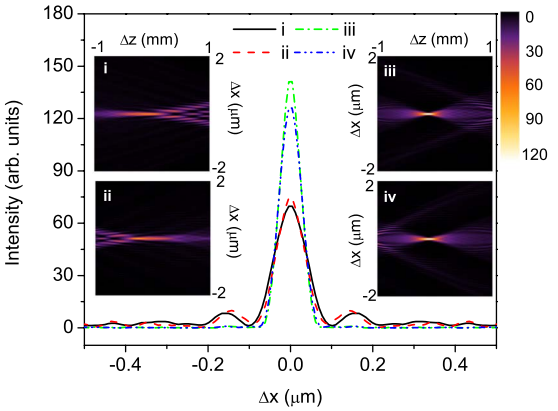

FIG. 10. (Color online) Focus profiles and intensity patterns around the focus (insets, intensity on linear scale) corresponding to the four cases shown in Fig. 9.

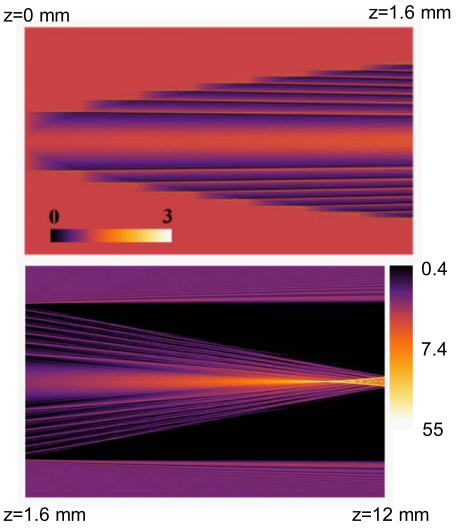

FIG. 11. (Color online) The wave field intensity distribution inside (top, intensity on linear scale) and after (bottom, intensity on logarithm scale) the KL in case i.

incident wave different from a plane wave will result in an aberration or shift of the focus. The bottom panel shows the intensity distribution after this KL. Apparently, the waves emerging from outer lens elements converge to a position different from the focus, leading to a much larger focus. This suggests that for such a long KL, its lens profile has to be modified to compensate the wave distortion incurred by the edge diffraction in a preceding element. A detailed discussion will be reported later. Short KLs with all elements lying in a single plane are much less affected by this effect because the wave distortion becomes severer as the wave propagates a longer distance. Regardless of all these drawbacks, the long KL shows only one single focus, a great advantage compared to short KLs where multiple foci are presented.

V. SUMMARY AND CONCLUSION

We conduct a comparative study on short and long KLs using the geometrical theory, the dynamical diffraction theory, and the beam-propagation method. The applicability and limitations of each method are discussed. We show that the result predicted by the geometrical theory deviates quickly from the one calculated by the more rigorous full-wave theories as the NA increases. Because of the large thickness needed for an integer multiple of 2π phase shift in a KL, the edge diffraction effect is more pronounced as compared to other diffractive optics. It is seen that for a KL with a relatively large physical NA and a large integer m, although the difficulty of fabrication is alleviated, it suffers not only a decrease in the efficiency but also a reduction in the effective NA. The study also shows that short KLs usually outperform long KLs in terms of efficiency and focal size because they are less affected by the edge diffraction effect. However, long KLs have only one focus, a great advantage compared to their short counterparts. For the conventional KLs studied in this paper, all show a focusing limit of tens of nanometers, larger than their diffraction-limited size. Adaptive lens design is suggested to reduce the wave field distortion associated with the strong-edge diffraction in a long KL and a further study is needed to find out the bottom limit.

ACKNOWLEDGMENT

This work was supported by the U.S. Department of Energy, Office of Science, Office of Basic Energy Sciences, under Contract No. DE-AC-02-98CH10886.

[1] H. C. Kang, J. Maser, G. B. Stephenson, C. Liu, R. Conley, A. T. Macrander, and S. Vogt, Phys. Rev. Lett. **96**, 127401 (2006).
[2] H. C. Kang *et al.*, Appl. Phys. Lett. **92**, 221114 (2008).
[3] S. Matsuyama *et al.*, Rev. Sci. Instrum. **77**, 103102 (2006).
[4] H. Mimura, Appl. Phys. Lett. **90**, 051903 (2007).
[5] C. G. Schroer *et al.*, Appl. Phys. Lett. **87**, 124103 (2005).
[6] Y. Suzuki *et al.*, Jpn. J. Appl. Phys. **44**, 1994 (2005).
[7] H. Yumoto *et al.*, Rev. Sci. Instrum. **76**, 063708 (2005).
[8] H. Yan, J. Maser, A. Macrander, Q. Shen, S. Vogt, G. B. Stephenson, and H. C. Kang, Phys. Rev. B **76**, 115438 (2007).
[9] L. Alianelli *et al.*, J. Synchrotron Radiat. **16**, 325 (2009).
[10] V. Aristov *et al.*, Appl. Phys. Lett. **77**, 4058 (2000).
[11] E. Di Fabrizio *et al.*, Nature (London) **401**, 895 (1999).
[12] K. Evans-Lutterodt, J. Ablett, A. Stein, C. Kao, D. Tennant, F. Klemens, A. Taylor, C. Jacobsen, P. Gammel, H. Huggins, G. Bogart, S. Ustin, and L. Ocola, Opt. Express **11**, 919 (2003).
[13] K. Evans-Lutterodt *et al.*, Phys. Rev. Lett. **99**, 134801 (2007).
[14] A. F. Isakovic *et al.*, J. Synchrotron Radiat. **16**, 8 (2009).
[15] D. A. Buralli, G. M. Morris, and J. R. Rogers, Appl. Opt. **28**, 976 (1989).
[16] D. Faklis and G. M. Morris, Appl. Opt. **34**, 2462 (1995).
[17] T. R. M. Sales and G. M. Morris, Appl. Opt. **36**, 253 (1997).
[18] F. Cerrina, J. Phys. D **33**, R103 (2000).

[19] Y. Chen G. Simon, A. M. Haghiri-Gosnet, F. Carcenac, D. Decanini, F. Rousseaux, and H. Launois, J. Vac. Sci. Technol. B **16**, 3521 (1998).
[20] J. Z. Y. Guo and F. Cerrina, IBM J. Res. Dev. **37**, 331 (1993).
[21] S. D. Hector, M. L. Schattenburg, and E. H. Anderson, J. Vac. Sci. Technol. B **10**, 3164 (1992).
[22] J. Van Roey, J. Vanderdonk, and P. E. Lagasse, J. Opt. Soc. Am. **71**, 803 (1981).